Many exciplex systems exhibit organic long-persistent luminescence

Naohiro Nishimura, Zesen Lin, Kazuya Jinnai, Ryota Kabe, and Chihaya Adachi**

N. Nishimura, Z. Lin, K. Jinnai, Prof. R. Kabe, Prof. C. Adachi
Center for Organic Photonics and Electronics Research (OPERA), Kyushu University
744 Motooka, Nishi-ku, Fukuoka 819-0395, Japan
E-mail: adachi@cstf.kyushu-u.ac.jp

N. Nishimura, Z. Lin, K. Jinnai, Prof. R. Kabe, Prof. C. Adachi
JST, ERATO Adachi Molecular Exciton Engineering Project
744 Motooka, Nishi-ku, Fukuoka 819-0395, Japan.

Prof. R. Kabe
Organic Optoelectronics Unit, Okinawa Institute of Science and Technology Graduate University
1919-1 Tancha, Onna-son, Kunigami-gun Okinawa, Japan 904-0495
E-mail: ryota.kabe@oist.jp

Prof. C. Adachi
International Institute for Carbon Neutral Energy Research (WPI-I2CNER), Kyushu University
744 Motooka, Nishi-ku, Fukuoka 819-0395, Japan.

Keywords: long-persistent luminescence, organic semiconductor, charge separation, charge recombination, exciplex

Abstract: Organic long-persistent luminescence (OLPL) is long-lasting luminescence from a photo-generated intermediated state, such as a charge separated state. Here, we show that many exciplex systems exhibit OLPL and that eminssion pathways of OLPL can be controlled by the relationship among local excited states and charge-transfer excited states of materials.

1. Introduction

Glow-in-the-dark materials exhibit continuous photoemission for a very long time. This long-lasting emission can originate as radioluminescence, photoluminescence, or chemiluminescence. Radioluminescent material has been known since the 20th century and was used for glow-in-the-dark paints because it emits continuously without photoexcitation.[1,2] However, because it contains radioactive elements, radioluminescent glow-in-the-dark material has gradually been replaced by long-persistence luminescent (LPL) materials based on photoluminescence.[1,2]

High-performance, LPL materials were developed in the mid 1990s, and are widely used for emergency lights and watches.[1-3] LPL systems all employ inorganic materials, and most of the high-performance materials require rare earth elements.[1-3] Moreover, inorganic materials generally require high fabrication temperatures.[1-3] Since inorganic LPL materials have no flexibility, they are dispersed into polymer media in large-scale applications.

The above problems can be solved by using organic light-emitting materials. Chemiluminescence results from a chemical reaction, and emission continues as long as the energy source molecule (usually organic peroxide) remains available.[4] Chemiluminescence systems comprising energy source molecules and organic emitters have been commercialized as chemical lights. Recently, a method for generating energy source peroxide species by photo-oxidation of semiconducting polymers has been reported, and it has been used for bioimaging (Figure 1).[4] However, chemiluminescent systems cannot sustain long-term use due to consumption of energy source agents.

Most organic photoluminescent materials showing long-lived emissions originate from phosphorescent materials. Although phosphorescence is often quenched by competing nonradiative processes, many organic systems having long-lived phosphorescence at room temperature have been reported.[5-10] However, phosphorescent emitters always exhibit exponential decay since there is no energy storage mechanism (Figure 1). In contrast, most LPL

systems exhibit power-law decay due to the presence of an intermediate charged state. Moreover, LPL duration is related to photo-excitation time because of a charge-storage mechanism, but normal phosphorescence does not depend on the photo-excitation time.[10]

The very first LPL emission from organic molecules was realized by dispersing an emitter molecule in a low-temperature polymer matrix under strong photo-excitation (Figure 1 (c)).[11] The emitter exhibits photo-induced ionization because of second photon absorption from the excited states. The slow charge recombination exhibits LPL emission from both singlet and triplet excited states. However, this successive two-photon ionization process requires high excitation power and a low-temperature environment.[12]

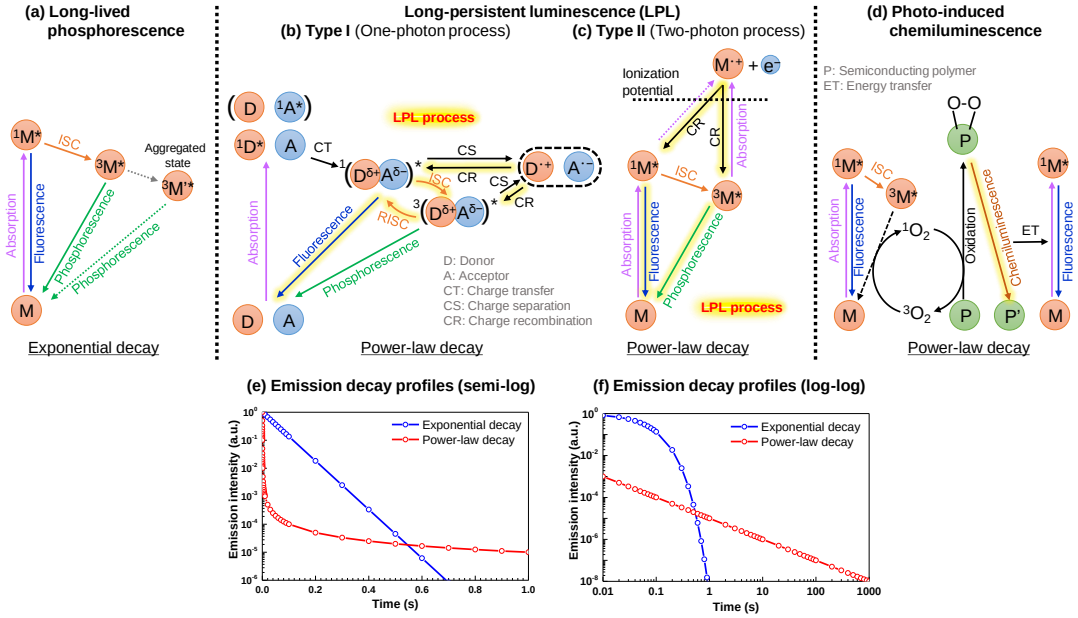

Figure 1. Classification of long-lasting emission from organic molecules. Power-law emission decay is essential for long-lasting emission over several minutes, as in commercial inorganic LPL systems. (a) Long-lived phosphorescence: emission from photo-generated triplet excited states (or lower triplet states generated by aggregation) to singlet ground states. (b) Long-persistent luminescence by one-photon absorption: emission from intermediate charge-separated states. Because the charge recombination process is a second order reaction, emission follows power-law decay. (c) Long-persistent luminescence by two-photon absorption: successive two-photon absorption ionizes the emitter. The recombination of electron and ionized molecule exhibits LPL emission. (d) Photo-induced chemiluminescence: A photo-sensitizer generates singlet oxygen and causes photo-oxidation of

a semiconducting polymer. Bond dissociation exhibits continuous chemiluminescence.. Semi-log (e) and log-log (f) plots of emission decay profiles.

Recently, we developed another organic LPL (OLPL) system exhibiting one-photon ionization, by mixing an electron donor *N*,*N*,*N'*,*N'*-tetramethylbenzidine (TMB) and an electron acceptor 2,8-bis(diphenylphosphoryl)dibenzo[b,d]thiophene (PPT) (Figure 1 (b)).[13-15] After photo-excitation of this OLPL system, an intermediate charge-separated state is generated by charge transfer from the electron donor to the acceptor. After turning off the photoexcitation, continuous charge-recombination produces LPL having a power-law emission decay.[16] This OLPL system can be fabricated not only using a low-temperature melt-casting method, but also thermal evaporation and spin-coating methods.[17] Moreover, the emission color of OLPL can be controlled by tuning the highest occupied molecular orbital (HOMO) level of the donor or energy transfer from exciplexes to extra-emitter dopants.[15,18] Furthermore, a transparent and flexible OLPL system can be realized by using a polymer-based acceptor.[19]

However, reported OLPL systems are few in number and the material selection rule for OLPL is still unclear. OLPL emission is based on exciplex, which is a transition from the lowest unoccupied molecular orbital (LUMO) of the acceptor to the highest occupied molecular orbital HOMO of the donor.[20-22] Therefore, the emission color of an OLPL system can be tuned with different combinations of donor and acceptor.[15,20] We also demonstrated that the lowest triplet-excited state of the donor significantly influences the emission mechanism.[14]

In this report, we systematically investigated LPL performance and physical properties of many donor and acceptor pairs, demonstrating the importance of the triplet-excited states of both the donor and acceptor for LPL emission.

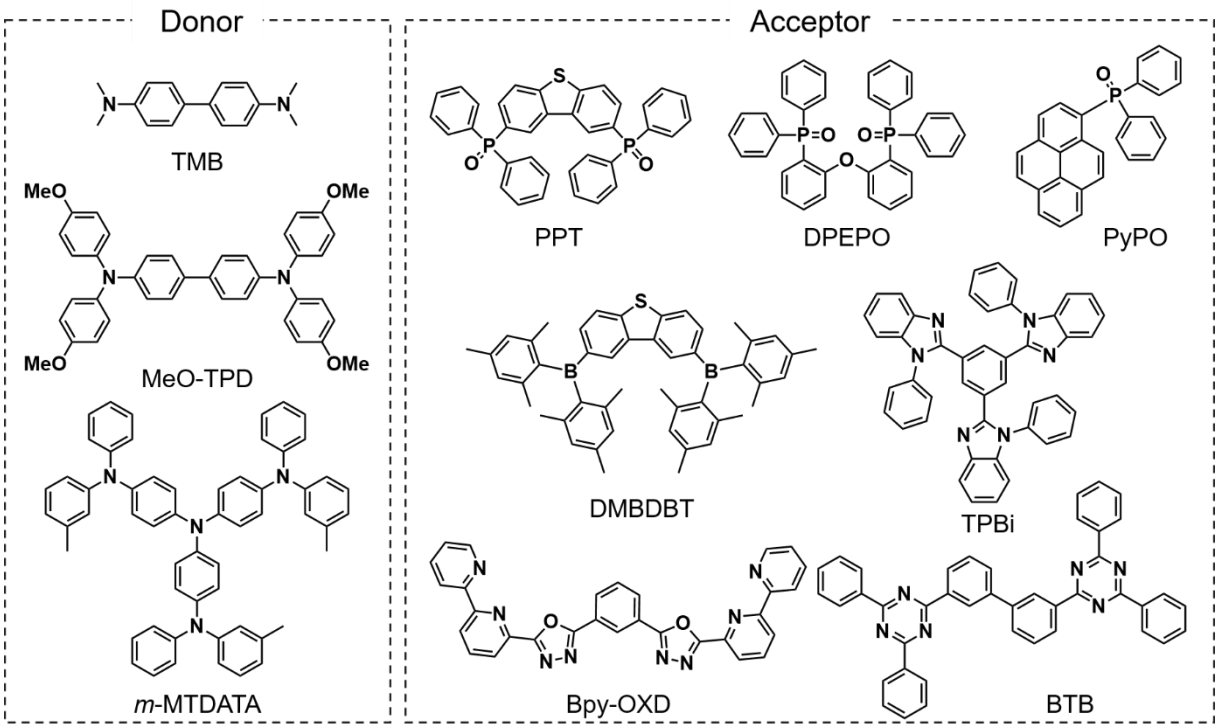

Figure 2. Chemical structures of electron donors and acceptors

2. Results and Discussion

2.1. Optical and electrical properties of electron donors and acceptors

Various electron donors and acceptors were investigated (Figure 2). TMB, 4,4',4"-tris[phenyl(*m*-tolyl)amino]triphenylamine (*m*-MTDATA), and *N*,*N*,*N'*,*N'*-tetrakis(4-methoxyphenyl)benzidine (MeO-TPD) were used as donors and PPT, diphenyl(1-pyrenyl)phosphine oxide (PyPO), 2,8-bis(2,4,6-trimesitylboronic)dibenzo[b,d]thiophene (DMBDBT), 3,3'-bis(4,6-diphenyl-1,3,5-triazin-2-yl)-1,1'-biphenyl (BTB), 1,3-bis[2-(2,2'-bipyridine-6-yl)-1,3,4-oxadiazo-5-yl]benzene (Bpy-OXD), 1,3,5-tris(1-phenyl-1H-benzimidazol-2-yl)benzene (TPBi), and bis[2-(diphenylphosphino)phenyl]ether oxide (DPEPO) were used as acceptors. Ultraviolet-visible (UV-Vis) absorption, fluorescence, and phosphorescence spectra of these materials are shown in Figure S1. Energy levels of the lowest triplet-excited states (T_1) were calculated from onsets of phosphorescence spectra obtained at 77 K. HOMO and LUMO levels were determined from the first oxidation or reduction peaks of cyclic voltammograms or differential-pulse voltammograms (Figure S2; Table 1).

Table 1. Optical properties of donors, acceptors, and exciplexes

Donor	Acceptor	HOMO (Donor) [eV][a]	LUMO (Acceptor) [eV][a]	$\Delta E_{HOMO-LUMO}$ [eV]	^1CT [eV][b]	^3LE_D [eV][c]	^3LE_A [eV][c]	E (^3LE_D-^1CT) [eV]	E (^3LE_A-^1CT) [eV]	PL peak [nm][d]	LPL peak [nm][d]	Φ_{PL} [%]	LPL duration time [s][e]
TMB	**PPT**	-4.65	-1.68	2.97	2.78	2.56	3.08	-0.22	0.30	522	527	6.5	868
MeO-TPD	**PPT**	-4.83	-1.68	3.15	2.94	2.56	3.08	-0.38	0.14	493(Sh.), 523	524	9.3	1073
***m*-MTDATA**	**PPT**	-4.58	-1.68	2.90	2.74	2.76	3.08	0.02	0.34	516	523	35.2	1352
***m*-MTDATA**	**TPBi**	-4.58	-1.84	2.74	2.70	2.76	2.80	0.06	0.10	546	557	16.6	110
***m*-MTDATA**	**DMBDBT**	-4.58	-2.05	2.53	2.68	2.76	3.00	0.08	0.32	525	N.D.	40.2	11
***m*-MTDATA**	**PyPO**	-4.58	-2.20	2.38	2.85	2.76	2.08	-0.09	-0.77	501	N.D.	52.1	N.D.
***m*-MTDATA**	**Bpy-OXD**	-4.58	-2.35	2.37	2.57	2.76	2.82	0.19	0.25	568	587	10.9	47
***m*-MTDATA**	**BTB**	-4.58	-2.32	2.26	2.48	2.76	3.01	0.28	0.53	575	N.D.	12.7	15
***m*-MTDATA**	**DPEPO**	-4.58	-1.54	3.04	3.03	2.76	3.52	-0.27	0.49	436	471	7.6	229

a. Calculated from redox peaks of cyclic voltammogram; *b*. Calculated from the onset of the exciplex emission spectra;
c. Calculated from the phosphorescence spectra obtained at 77 K; *d*. Obtained from Figure S3; *e*. Time until the emission intensity drops below 3 pW.

Mixed films with a 1:99 molar ratio of donor/acceptor were fabricated using a melt-cast method, from which steady-state photoluminescence and LPL spectra, emission decay profiles, and emission quantum yields (Φ_{PL}) were obtained (Figures 3 and 4). In this study, the ^3CT level of exciplex is assumed from the ^1CT level of exciplex obtained at the onset of steady-state photoluminescence spectra, because there is no method to measure the ^3CT of exciplex directly. Many exciplex systems have very small energy gap between the ^1CT and the ^3CT because the HOMO is localized on donor and LUMO is localized on accepter, which lead to small exchange energy.[20]

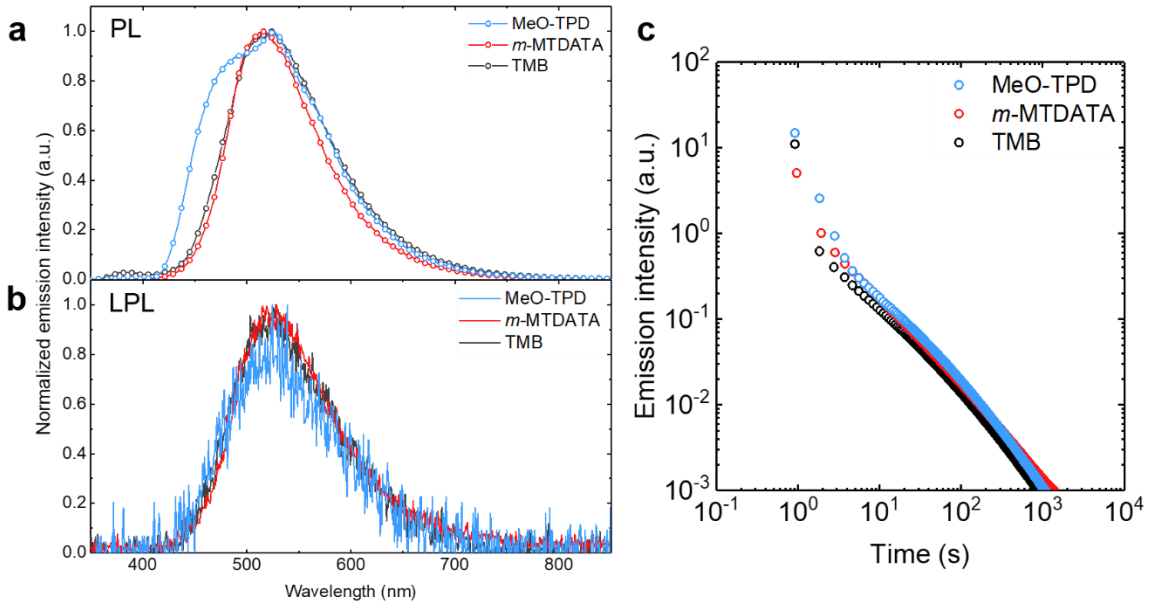

Figure 3. PL (a) and LPL (b) spectra and LPL emission decay (c) of MeO-TPD/PPT, *m*-MTDATA/PPT, and TMB/PPT. Charge transfer (CT) emission corresponding to $\Delta E_{HOMO-LUMO}$. LPL spectra was changed when ^3LE_D is much lower than ^1CT (MeO-TPD/PPT).

2.2. Donor-dependence of LPL performance

When PPT was used as the acceptor, all films (TMB/PPT, *m*-MTDATA/PPT, and MeO-TPD/PPT) exhibited broad exciplex emission, corresponding to a transition from LUMO of the acceptor to HOMO of the donor (Figure 3). Because the TMB/PPT and *m*-MTDATA/PPT films have almost the same energy gap between donor HOMO and acceptor LUMO ($\Delta E_{HOMO-LUMO}$ = 2.97 and 2.90 eV, respectively), both films exhibited similar photoluminescence and LPL spectra. However, the *m*-MTDATA/PPT system exhibited ~1.5× longer emission because its Φ_{PL} was higher than that of TMB/PPT. Similar correlations between the Φ_{PL} and LPL duration have been reported in previous reports[15,18]. Because the MeO-TPD/PPT film had a larger energy gap ($\Delta E_{HOMO-LUMO}$ = 3.15 eV), it exhibited two emission peaks at 493 nm (shoulder peak) and 523 nm in the steady-state photoluminescence spectrum and a single peak at 523 nm in the LPL spectrum. Because the LPL spectrum corresponds to the phosphorescence of MeO-TPD (Figure S3), the PL peak at 493 nm represents the exciplex emission between MeO-TPD

and PPT. However, the LPL decay of MeO-TPD follows power-law decay unlike conventional phosphorescence emitters showing exponential decay.

The LPL of MeO-TPD/PPT can be explained by electron transfer in the triplet-excited states (Figure 5). In the case of TMB/PPT and *m*-MTDATA/PPT systems, the energy gap between the ^{1}CT and the lowest triplet-excited state of the donor (^{3}LE$_D$), $\Delta E(^1\text{CT} - {}^3\text{LE}_D)$, is very small (0.22 and −0.02 eV, respectively) (Figure S4). Therefore, the reverse intersystem crossing (RISC) from ^{3}LE$_D$ to ^{1}CT is efficient, as in thermally activated delayed fluorescence (TADF) molecules.[23-26] As a result, excitons generated by charge recombination are mainly populated on the ^{1}CT and exhibit LPL from the exciplex. In contrast, MeO-TPD/PPT has a rather large energy gap between $\Delta E(^1\text{CT} - {}^3\text{LE}_D)$ = 0.38 eV, which almost prevents the RISC process. Therefore, both transitions from ^{1}CT and ^{3}LE$_D$ are present in PL (Figure S5). After charge recombination, excitons populate mainly ^{3}LE$_D$ through electron transfer and exhibit LPL emission from ^{3}LE$_D$. ^{3}LE$_D$ is usually emissive in OLPL system because the donor molecule is isolated in a rigid acceptor matrix having high triplet energy.[10] Therefore, a small $\Delta E(^1\text{CT} - {}^3\text{LE}_D)$ is required for efficient LPL emission.

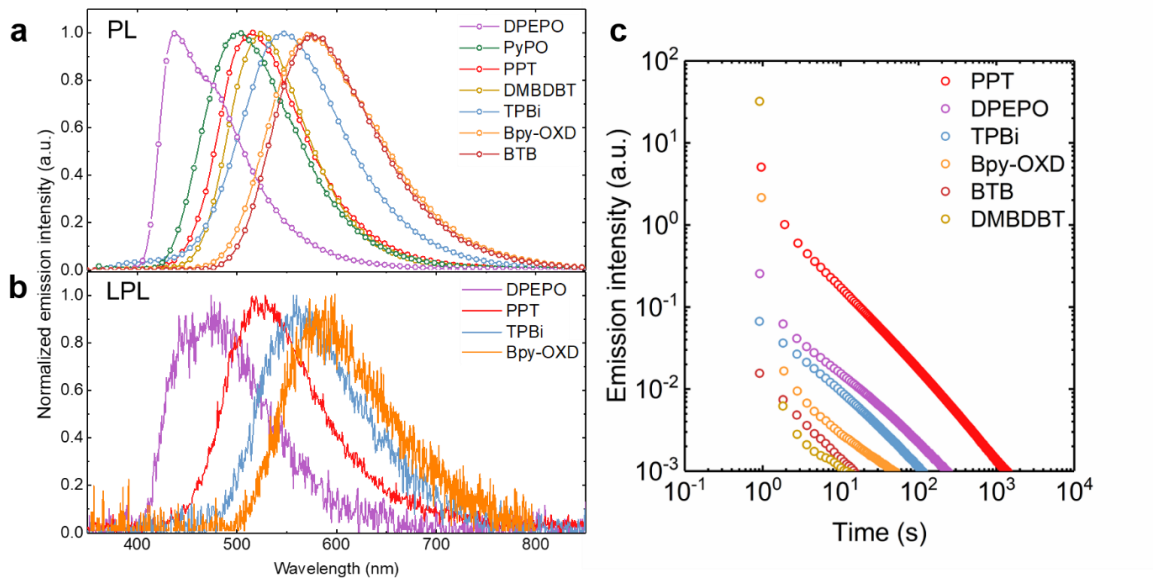

Figure 4. PL (a) and LPL (b) spectra and LPL emission decay (c) of *m*-MTDATA/Acceptor (DPEPO, PPT, DMBDBT, PyPO, TPBi, Bpy-OXD, and BTB). Sky-blue to orange exciplex emission was observed, corresponding to various $\Delta E_{\text{HOMO-LUMO}}$.

2.3. Accepor-dependence of LPL performance

Subsequently, when *m*-MTDATA was used as the donor, all combinations of *m*-MTDATA/Acceptor (DPEPO, PPT, DMBDBT, PyPO, TPBi, Bpy-OXD, and BTB) exhibited exciplex emission (Figure 4). Sky-blue to orange exciplex emission was observed corresponding to various $\Delta E_{HOMO-LUMO}$ of donor and acceptor combinations. Emission decay profiles of all films except *m*-MTDATA/PyPO follow power-law decay, which is characteristic of LPL emission. LPL spectra of *m*-MTDATA/DMBDBT and *m*-MTDATA/BTB are not presented in Figure 4b, since their LPL intensities were too weak to be detected.

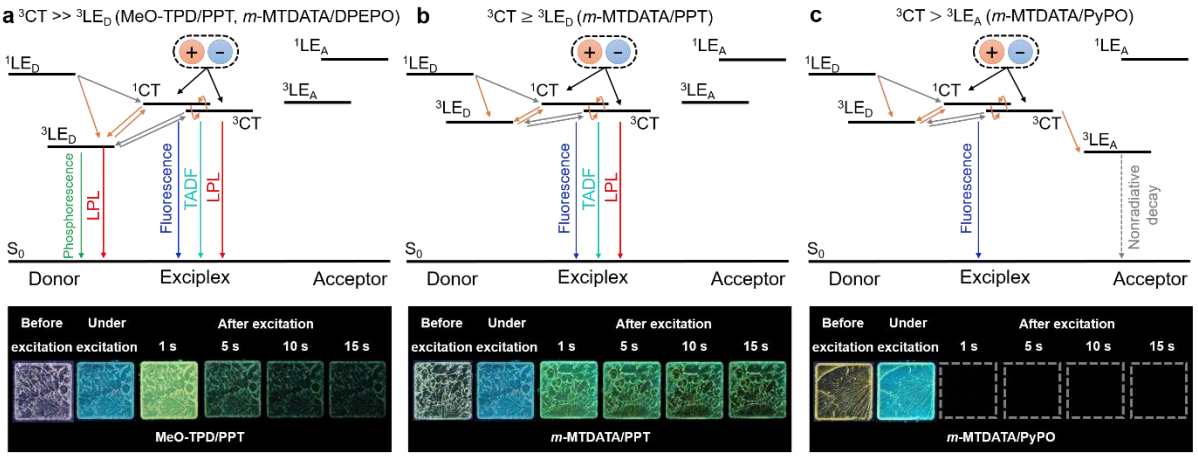

Figure 5. Proposed emission mechanism and photograph of OLPL (a) When $^3CT >> {}^3LE_D$. (b) $^3CT \geq {}^3LE_D$ (c) $^3CT > {}^3LE_A$. Energy level relationships among ^3LE_A, ^3LE_D, and ^1CT are important to control the emission pathway after charge recombination.

In the case of the *m*-MTDATA/PyPO system, LPL emission was quenched by electron transfer because the triplet energy level of PyPO (^3LE_A) is much lower than that of the exciplex (^3CT). Excitons generated by charge recombination are transferred to the non-emissive ^3LE_A state.

The *m*-MTDATA/DPEPO system shows spectral changes between PL and LPL spectra similar to those of the MeO-TPD/PPT system (Figure S6). Because ^3LE_D is lower than ^1CT, LPL is mainly obtained from ^3LE_D. Notably, the *m*-MTDATA/DMBDBT system exhibits

strong degradation during photo-excitation (Figure S7). The unstable radical anion of DMBDBT might cause this photo-degradation after the charge-separation process.

These results identify several important factors for developing efficient OLPL systems. When the energy level of ^{1}CT is lowest or slightly higher (< 0.3 eV) than that of ^3LE_D and ^3LE_A, the mixture of donor and acceptor exhibits LPL from ^{1}CT (fluorescence-based LPL). When ^3LE_D is enough lower than ^{1}CT, LPL emission is mainly obtained from emissive ^3LE_D, since the donor is in a rigid acceptor matrix (phosphorescence-based LPL). When ^3LE_A is lowest, LPL is quenched because ^3LE_A is usually non-emissive due to competing nonradiative decay. When LPL emission is obtained from the exciplex, LPL emission color corresponds to the $\Delta E_{HOMO-LUMO}$ and emission intensity corresponds to Φ_{PL} of the exciplex. The radical cation state of donors and the radical anion state of acceptors must be stable to avoid photo-decomposition.

3. Conclusions

In conclusion, we demonstrated that many exciplex systems exhibit LPL emission. The emission color of OLPL corresponds to the energy gap between donor HOMO and acceptor LUMO. To design efficient OLPL systems, energy level relationships among ^3LE_A, ^3LE_D, and ^{1}CT are important for controlling the emission pathway after charge recombination. Φ_{PL} of the exciplex and redox stabilities of the materials are also key factors. This information will enable development of efficient, full-color OLPL systems involving not only small molecules, but also polymers.

Experimental Section

Materials: PPT [27], DPEPO [28] , PyPO [29] , DMBDBT [30], and BTB [31] were prepared as described in the literature, while TMB, MeO-TPD, *m*-MTDATA, TPBi and Bpy-OXD were obtained from TCI Chemicals (Tokyo, Japan) or Luminescence Technology Corp. (Taipei, Taiwan) and purified by sublimation.

Film fabrication: In a nitrogen-filled glovebox, mixtures of donors and acceptors were placed on template glass substrates with a surface area of 100 mm^2 and a depth of 0.5 mm, whereupon they were heated to 250° C for 10 s. After melting, substrates were rapidly cooled to room temperature.

Optical and electrical Measurements: Absorption spectra were measured using a UV-vis-NIR spectrophotometer (LAMBDA 950, Perkin Elmer). Photoluminescence spectra were measured using spectrofluorometers (FluoroMax, Horiba Jobin Yvon; FP-8600, JASCO; and PMA-12, Hamamatsu Photonics). Absolute photoluminescence quantum yields (Φ_{PL}) were measured using an integrating sphere with a photoluminescence measurement unit (Quantaurus-QY, Hamamatsu Photonics).

Cyclic voltammetry measurements were carried out using an electrochemical analyzer (Model 608D+DPV, BAS). Measurements were performed in dried and oxygen-free DMF using 0.1 M tetrabutylammonium hexafluorophosphate as a supporting electrolyte. A platinum fiber was used as a counter electrode, with glassy carbon as a working electrode, and Ag/Ag^+ as a reference electrode. Redox potentials were referenced against ferrocene/ferrocenium (Fc/Fc^+). Corresponding LUMO energies were calculated from reduction peaks using an absolute value of −4.8 eV to vacuum for the Fc/Fc^+ redox potential.

LPL Measurements: LPL properties (spectra and decay profiles) were obtained using a measurement system in a glove box. Fabricated films were placed in the dark box and excited using a 340-nm LED (M340L4, Thorlabs) with a band pass filter (340 ± 5 nm) at a fixed excitation power (100 μW cm^{-2}). PL and LPL spectra were recorded using a multichannel spectrometer (QE-Pro, Ocean Photonics). Emission decay profiles were obtained without wavelength sensitivity calibration using a silicon photomultiplier (C13366-1350GA, Hamamatsu Photonics) connected to a multimeter (34461A, Keysight).

Supporting Information

Supporting Information is available from the Wiley Online Library or from the author.

Acknowledgements

This work was supported by the Japan Science and Technology Agency (JST), ERATO, Adachi Molecular Exciton Engineering Project, under JST ERATO Grant Number JPMJER1305, Japan, the International Institute for Carbon Neutral Energy Research (WPI-I2CNER) sponsored by the Ministry of Education, Culture, Sports, Science and Technology (MEXT), JSPS KAKENHI Grant Numbers JP18H02049 and JP18H04522, and the Mitsubishi Foundation.

Received: ((will be filled in by the editorial staff))
Revised: ((will be filled in by the editorial staff))
Published online: ((will be filled in by the editorial staff))

References

[1] S. Wu, Z. Pan, R. Chen, X. Liu, *Long Afterglow Phosphorescent Materials*, Springer Nature Switzerland AG. **2017**.
[2] J. Xu, S. Tanabe, *J. Lumin.* **2019**, 205, 581.
[3] Y. Li, M. Gecevicius, J. Qiu, *Chem. Soc. Rev.* **2016**, 45, 2090.
[4] Q. Miao, C. Xie, X. Zhen, Y. Lyu, H. Duan, X. Liu, J. V. Jokerst, K. Pu, *Nat. Biotechnol.* **2017**, 35, 1102.
[5] S. Hirata, *Adv. Opt. Mater.* **2017**, 5, 1700116.
[6] S. Xu, R. Chen, C. Zheng, W. Huang, *Adv. Mater.* **2016**, *28*, 9920.
[7] A. Forni, E. Lucenti, C. Botta, E. Cariati, *J. Mater. Chem. C* **2018**, *6*, 4603.
[8] C. Chen, B. Liu *Nat. Commun.* **2019**, *10*, 2111.
[9] S. Hirata, K. Totani, J. Zhang, T. Yamashita, H. Kaji, S. R. Marder, T. Watanabe, C. Adachi, *Adv. Funct. Mater.* **2013**, *23*, 3386.
[10] N. Notsuka, R. Kabe, K. Goushi, C. Adachi, *Adv. Funct. Mater.* **2017**, *27*, 1703902.
[11] H. Ohkita, W. Sakai, A. Tsuchida, M. Yamamoto, *Macromolecules* **1997**, 30, 5376.
[12] H. Ohkita, W. Sakai, A. Tsuchida, M. Yamamoto, *Bull. Chem. Soc. Jpn.* **1997**, 70, 2665.
[13] R. Kabe, C. Adachi, *Nature* **2017**, 550, 384.
[14] Z. Lin, R. Kabe, K. Wang, C. Adachi, *Nat. Commun*. **2020**, 11, 191.
[15] Z. Lin, R. Kabe, C. Adachi, *Chem. Lett*. **2020**, 49, 203.
[16] P. Debye, J. Edwards, *J. Chem. Phys.* **1952**, 20, 236.
[17] K. Jinnai, N. Nishimura, R. Kabe, C. Adachi, *Chem.Lett*. **2019**, 48, 270.
[18] K. Jinnai, R. Kabe, C. Adachi, *Adv. Mater.* **2018**, 30, 1800365.
[19] Z. Lin, R. Kabe, N. Nishimura, K. Jinnai, C. Adachi, *Adv. Mater.* **2018**, 30, 1870341.
[20] M. Sarma, K.-T. Wong, *ACS Appl. Mater. Interfaces* **2018**, *10*, 19279.
[21] P. B. Deotare, W. Chang, E. Hontz, D. N. Congreve, L. Shi, P. D. Reusswig, B. Modtland, M. E. Bahlke, C. K. Lee, A. P. Willard, V. Bulović, T. Van Voorhis, M. A. Baldo, *Nat. Mater.* **2015**, *14*, 1130.
[22] W. Chang, D. N. Congreve, E. Hontz, M. E. Bahlke, D. P. McMahon, S. Reineke, T. C. Wu, V. Bulović, T. Van Voorhis, M. A. Baldo, *Nat. Commun.* **2015**, *6*, 6415.
[23] H. Uoyama, K. Goushi, K. Shizu, H. Nomura, C. Adachi, *Nature* **2012**, *492*, 234.
[24] K. Goushi, K. Yoshida, K. Sato, C. Adachi, *Nat. Photonics* **2012**, *6*, 253.
[25] K. Goushi, C. Adachi, *Appl. Phys. Lett.* **2012**, 101, 023306**.**
[26] H. Noda, H. Nakanotani, C. Adachi, *Sci. Adv.* **2018**, 4, eaao6910.

[27] C. Fan, C. Duan, Y. Wei, D. Ding, H. Xu, W. Fuang, *Chem. Mater*. **2015**, 27 5131.
[28] K. Miyata, T. Nakagawa, R. Kawakami, Y. Kita, K. Sugimoto, T. Nakashima, T. Harada, T. Kawai, Y. Hasegawa, *Chem. Eur. J.* **2011**, 17. 521.
[29] Q. Fang, G. Yang, *Chem. Commun.* **2017**, 53, 5702.
[30] L. Wang, Y. Fang, H. Mao, Y. Qu, J. Zuo, Z. Zhang, G. Tan, X. Wang, *Chem. Eur. J.* **2017**, 23, 6930.
[31] C. S. Oh, Y. J. Kang, S. K. Jeon, J. Y. Lee, *J. Phys. Chem. C* **2015**, 119, 22618.

Keyword long-persistent luminescence, organic semiconductor, charge separation, charge recombination, exciplex

Naohiro Nishimura, Zesen Lin, Kazuya Jinnai, Ryota Kabe*, and Chihaya Adachi*

Many exciplex systems exhibit organic long-persistence luminescence

ToC figure

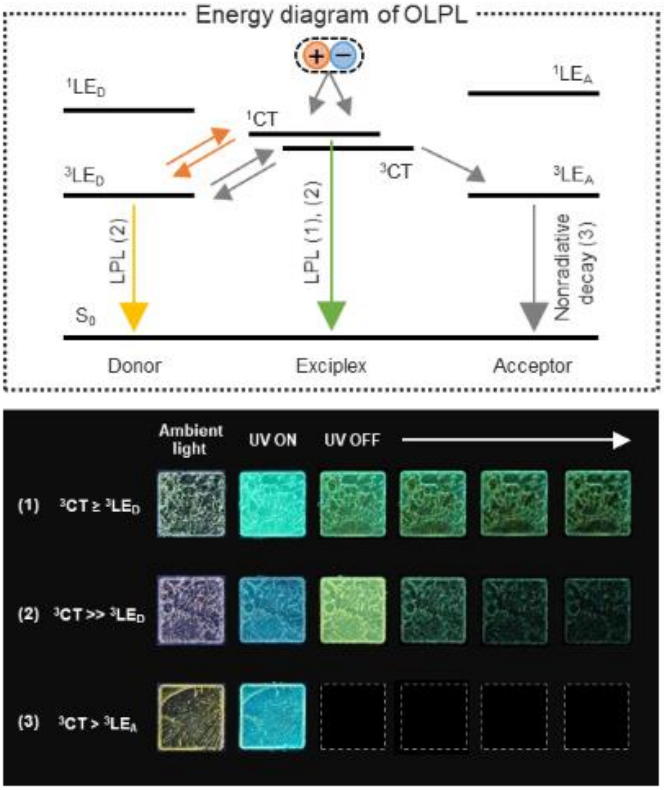

Organic long-persistent luminescence (OLPL) is long-lasting luminescence from a photo-generated intermediated state. Here, we show that many exciplex systems exhibit OLPL and that eminssion pathways of OLPL can be controlled by the relationship among local excited states (^3LE_D and ^3LE_A) and charge-transfer excited states (^3CT) of materials.

Supporting Information

Many organic exciplex systems exhibit long-persistence luminescence

Naohiro Nishimura, Zesen Lin, Kazuya Jinnai, Ryota Kabe, Chihaya Adachi**

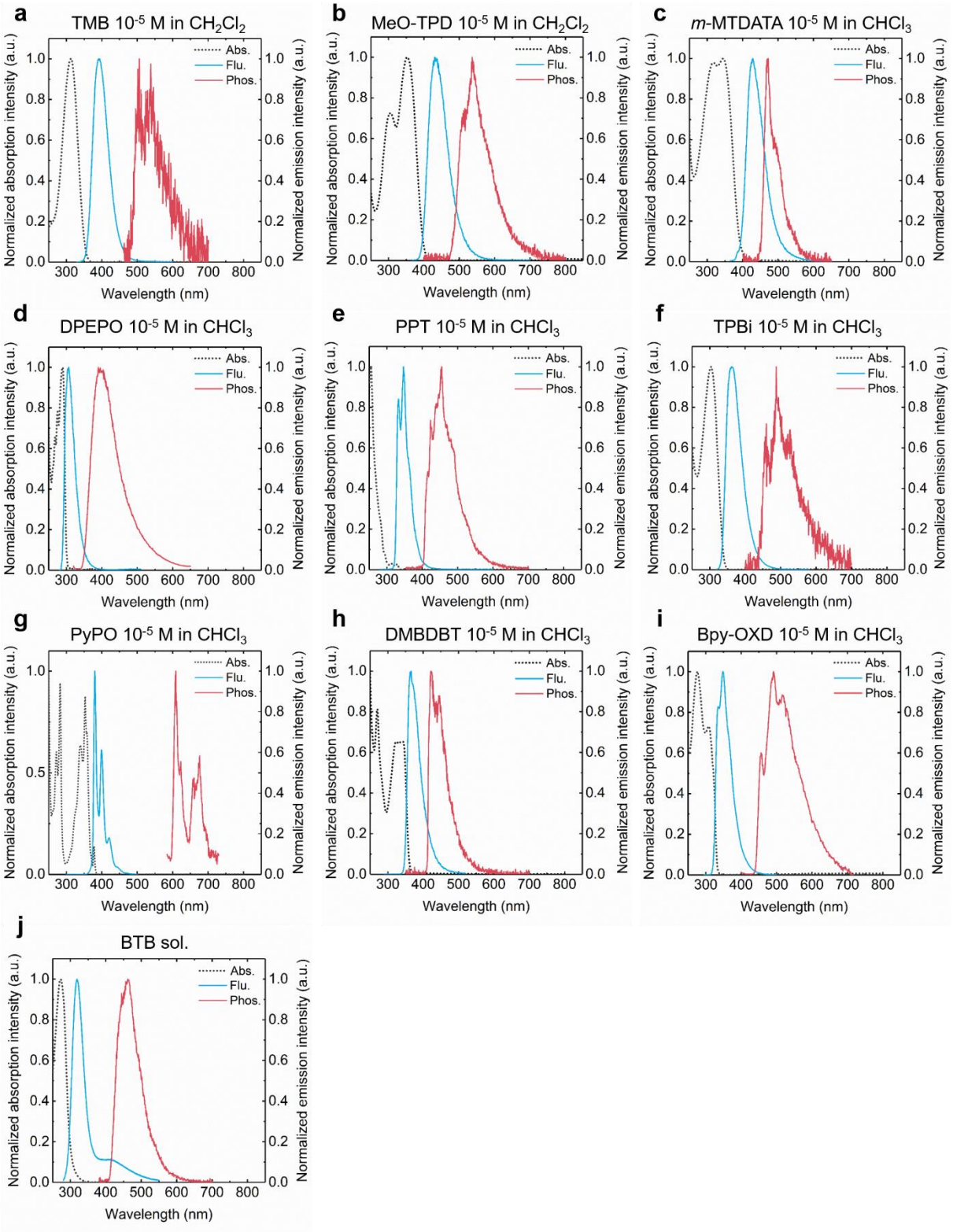

Figure S1. Local excited energy levels of donors and acceptors (^1LE_D, ^3LE_D, ^1LE_A, and ^3LE_A) were obtained from solution-state emission spectra. UV-vis absorption, fluorescence, and phosphorescence spectra of the donors and acceptors in solution. Phosphorescence spectra were obtained at 77 K.

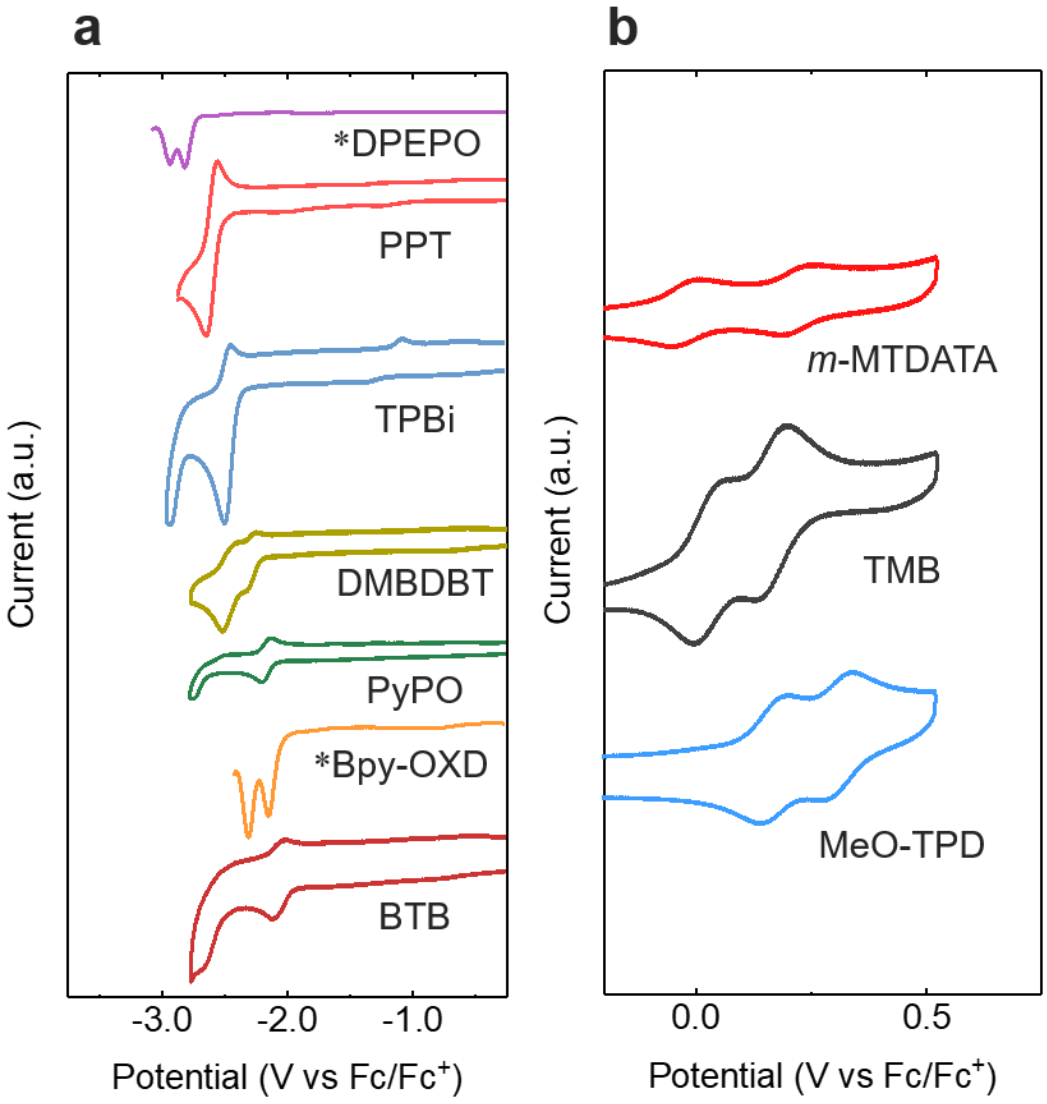

323

324 **Figure S2.** Donor HOMO and acceptor LUMO levels were calculated from cyclic voltammograms (or

325 *differential pulse voltammogram) of acceptors (a) and donors (b).

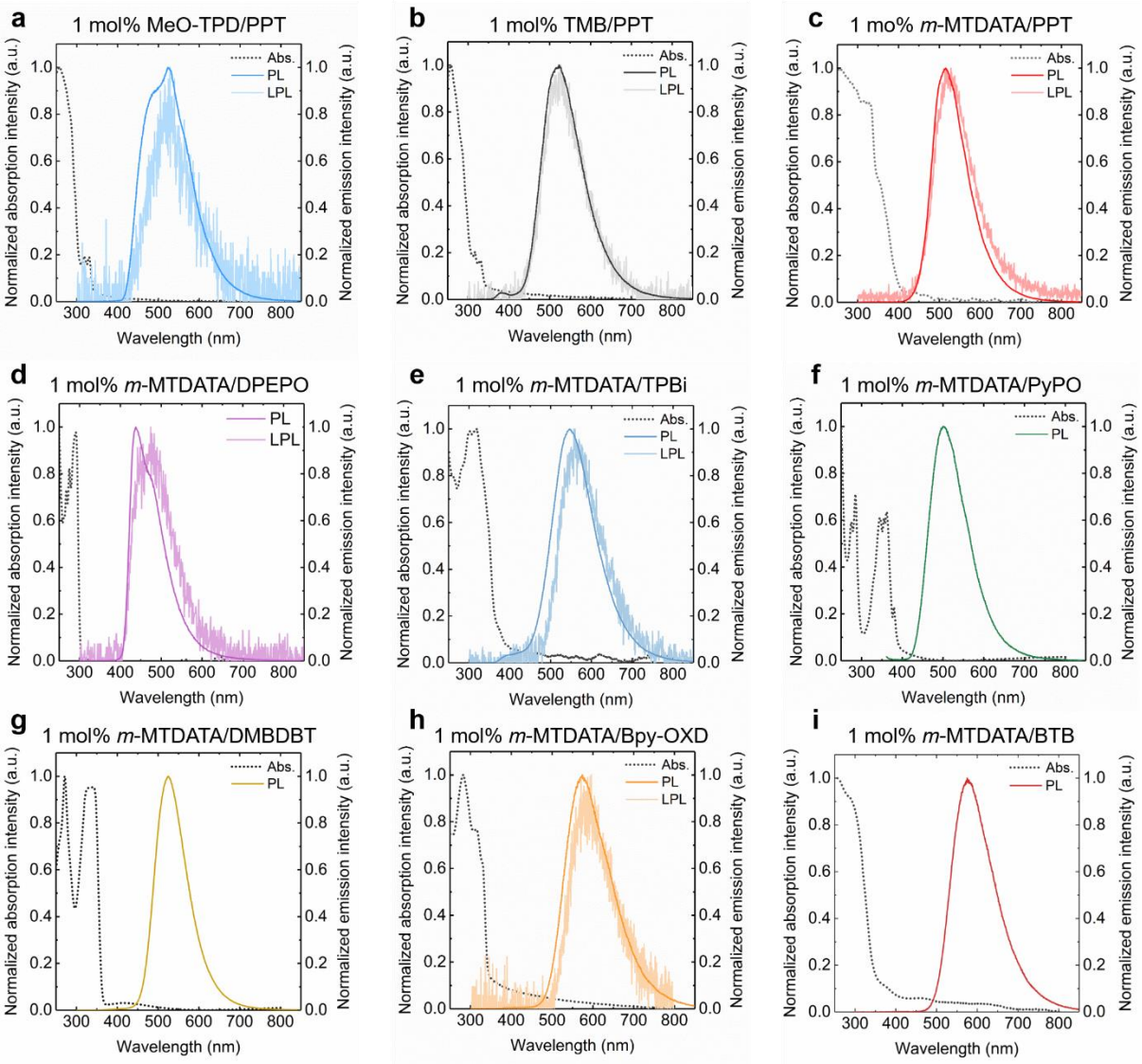

Figure S3. Comparison between steady-state photoluminescence (PL) and LPL spectra of all films. When $\Delta E(^1\mathrm{CT} - {}^3\mathrm{LE_D})$ is large, LPL spectra are changed from PL spectra (a,d). When $\Delta E(^1\mathrm{CT} - {}^3\mathrm{LE_D})$ is very small, PL and LPL spectra are almost identical (b,c,e,h). When $\Delta E(^1\mathrm{CT} - {}^3\mathrm{LE_A})$ is large, LPL is quenched (f). LPL intensities were too weak to be detected (g, i)

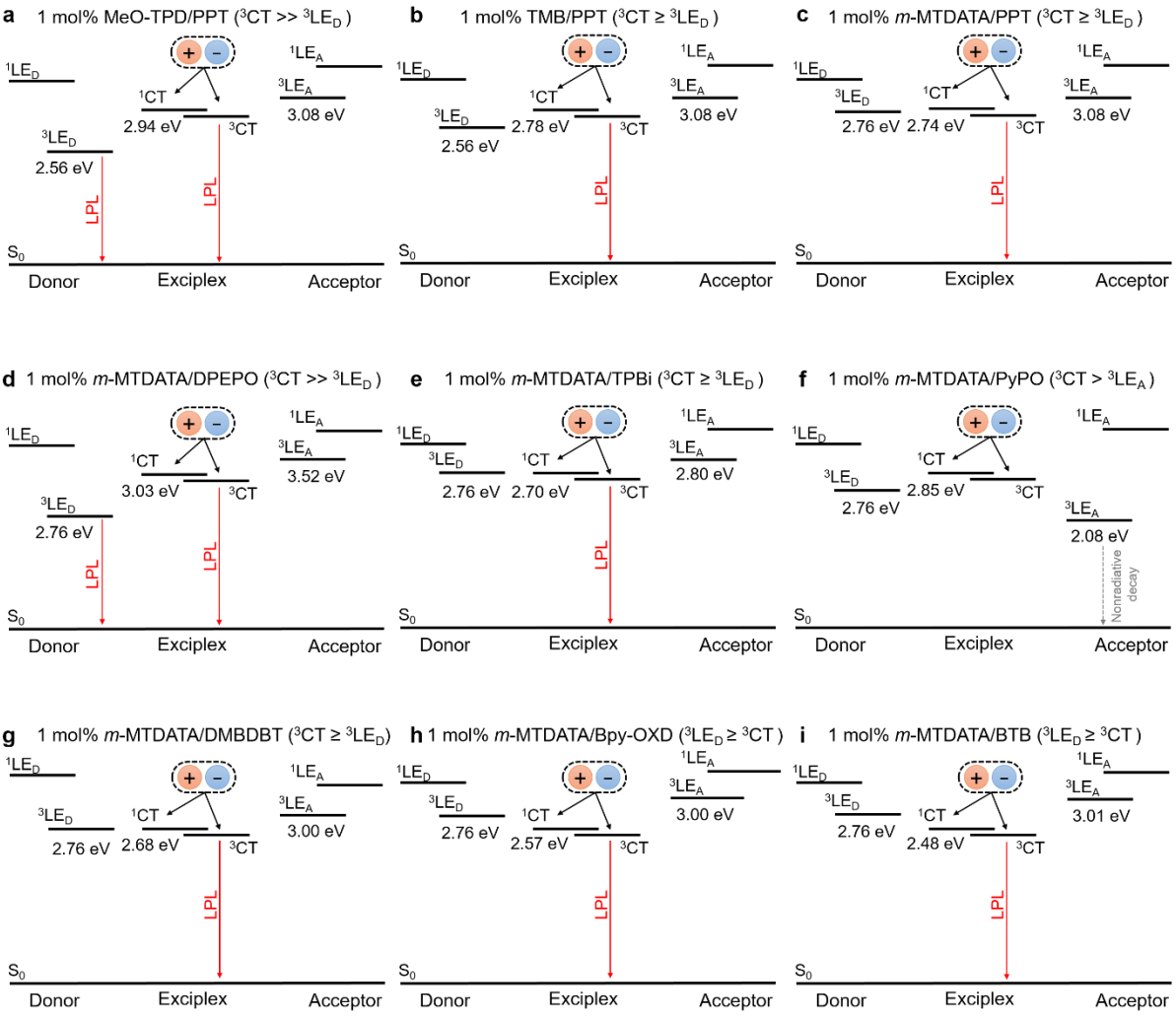

Figure S4. The energy-level-relationship for all the exciplex couples

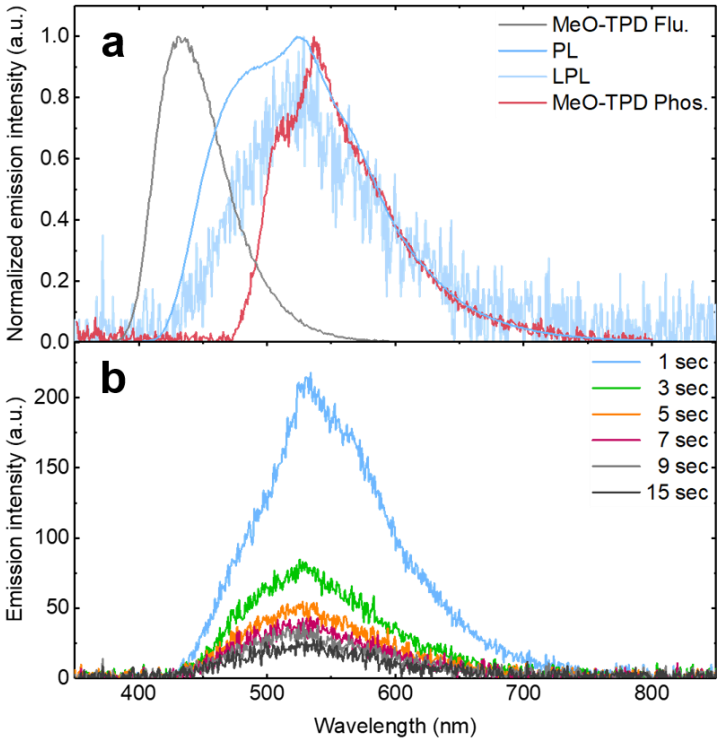

Figure S5. Time-dependent spectral shifting of an MeO-TPD/PPT film from PL (transition from ^3LE_D and ^1CT) to LPL (transition from ^1CT). (a) Fluorescence and phosphorescence spectra of MeO-TPD, and PL and LPL spectra of MeO-TPD/PPT film. (b) Time-dependent emission spectra of MeO-TPD/PPT film.

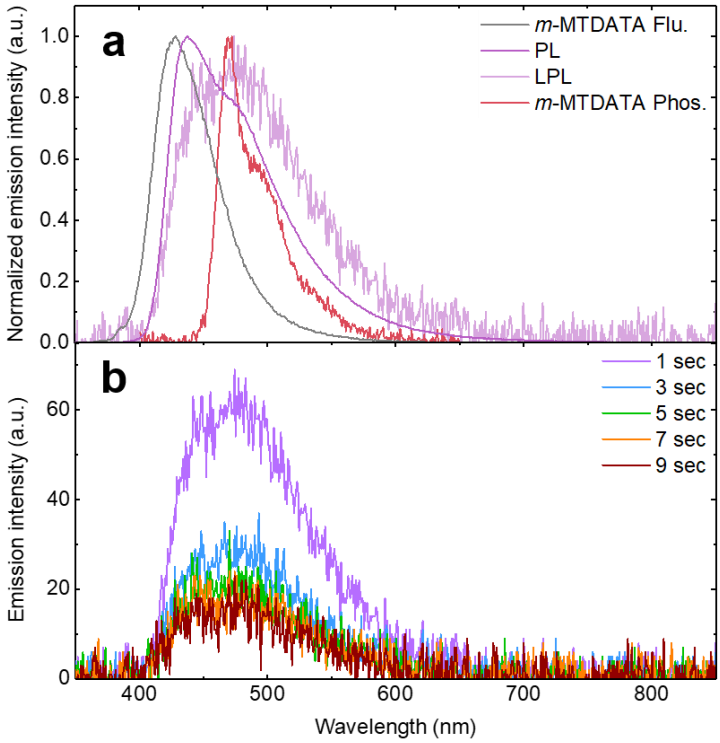

Figure S6. Time-dependent spectral shifting of a *m*-MTDATA/DPEPO film from PL (transition from ^3LE_D and ^1CT) to LPL (transition from ^1CT). (a) Fluorescence and phosphorescence spectra of *m*-MTDATA and PL and LPL spectra of *m*-MTDATA/DPEPO film. (b) Time-dependent emission spectra of a *m*-MTDATA/DPEPO film.

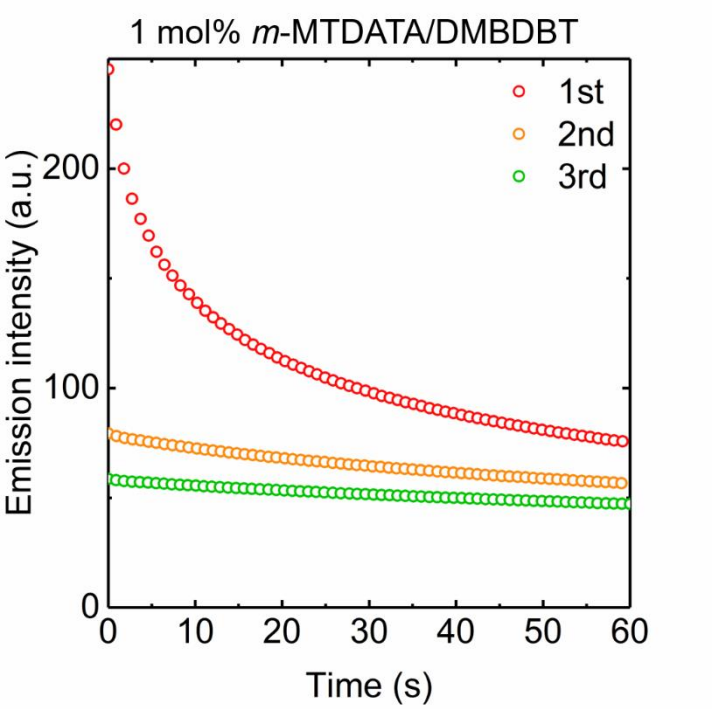

Figure S7. Photo-degradation of a *m*-MTDATA/DMBDBT film. Emission intensity diminishes during photo-irradiation (60 s) of *m*-MTDATA/DMBDBT film with repeated measurements.